A Compensation Component Injection Method Based on a Hybrid Modulation for Minimizing the Neutral-Point Voltage Oscillations in a Five-Level Flying Capacitor Rectifier

Peng Zhang, Xuezhi Wu, *Member, IEEE*, Wenzheng Xu, Jingdou Liu, Jingjing Qi, and Anna Yang

***Abstract*—Neutral-point (NP) voltage oscillating is an inherent problem for multilevel converters with split dc-link capacitors. In this article, a compensation component injection method based on a hybrid modulation for minimizing the NP voltage oscillations in a five-level flying capacitor rectifier is proposed. In specific, the equivalent modulation waves are first obtained by adopting an existing simplified space-vector modulation method. And a hybrid modulation which gives both the same optimal harmonic performance as phase-disposition pulse width modulation (PWM) and the same superiority of flying capacitor voltage regulation as phase-shifted PWM is adopted. Meanwhile, the solved optimal compensation component in each subsector is injected to make the average NP current equal to zero for minimizing the NP voltage oscillations. Simulations and experiments were conducted to verify the performance of the proposed compensation method based on the hybrid modulation.**

***Index Terms*—Compensation component injection, five-level flying capacitor (5L-FC) rectifier, hybrid modulation, neutral-point (NP) voltage oscillations minimization, phase-disposition pulsewidth modulation (PDPWM), phase-shifted PWM (PSPWM), simplified carrier-based space-vector modulation (SVM) method.**

I. Introduction

FOR SOME nonregenerative power applications, such as dc charger systems, wind energy conversion systems, power factor corrections, telecommunications, aircrafts, etc., multilevel unidirectional rectifiers are being preferred, as they use less active switches, which helps to increase power density, reduce system cost and improve reliability [1]–[5]. Different multilevel rectifiers have been proposed in [6]–[13], which are hybrids and modifications of conventional multilevel topologies including diode clamp type, flying capacitor (FC) type, and cascaded h-bridge type. Among them, one superior topology [7] composed of diode clamp type and FC type is shown in Fig. 1. Only four switches and four diodes are needed in each phase leg to generate five voltage levels.

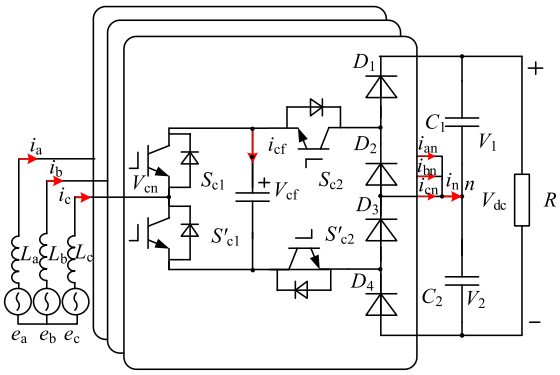

Fig. 1. Topology of the 5L-FC rectifier.

In practical applications, the capacitor voltage balancing, including three FCs and two dc-link capacitors, is of great importance. Capacitor voltage imbalance not only increases voltage stress on switches and capacitors, which reduces their operational lifetime and reliability, but also has a negative impact on the fundamental component of the input currents with increasing current total harmonic distortion (THD). At present, a large number of modulation strategies have been proposed to address the problem, which can be mainly categorized into carried-based pulsewidth modulation (PWM) methods [14]–[18], space-vector PWM (SVPWM) techniques [19]–[22], and other modulation strategies [23]–[27].

Carrier-based PWM is easy to be implemented with low calculation complexity. PSPWM [14] is widely used in multilevel converters, for its convenience and capability of natural FC voltage balance. The FC voltages are regulated by slightly adjusting the two modulation waves while the dc-link voltage balancing is achieved by injecting zero-sequence component. PDPWM [15] has better line voltage harmonic performance. However, the conduction and switching losses are distributed nonuniformly. The FC voltage and dc-link voltage are balanced by choosing

Manuscript received February 24, 2021; revised May 30, 2021 and August 6, 2021; accepted September 12, 2021. Date of publication September 21, 2021; date of current version November 30, 2021. This work was supported by the National Key R&D Program of China under Grant 2019YFE0100300. Recommended for publication by Associate Editor F. Wang. *(Corresponding author: Xuezhi Wu.)*

The authors are with the School of Electrical Engineering, Beijing Jiaotong University, Beijing 100044, China (e-mail: 20117034@bjtu.edu.cn; xzhwu@bjtu.edu.cn; xuwenzheng@bjtu.edu.cn; jdliu@bjtu.edu.cn; 18117016@bjtu.edu.cn; 19121515@bjtu.edu.cn).

Color versions of one or more figures in this article are available at https://doi.org/10.1109/TPEL.2021.3113947.

Digital Object Identifier 10.1109/TPEL.2021.3113947

suitable redundant switching states and injecting suitable zero-sequence voltage respectively. Some improved PSPWM and hybrid modulation schemes are also proposed in [16]–[18] to combine the advantages of PSPWM and PDPWM. Comparatively, SVPWM has a better performance with high utilization of dc voltages and flexibility. In [19], an optimized SVPWM strategy in the virtual coordinate is proposed. All triangles in the five-level space vector diagram (5L-SVD) are divided into seven categories which have different characteristics of balancing the neutral-point (NP) potential. In [20], a novel SVPWM algorithm based on line voltage coordinate is studied for reducing the calculations. The voltage balancing of dc-link capacitors and FC capacitors are realized by choosing suitable switching sequence and redundant switching states. In [21] and [22], for the aim of reducing the common-mode voltage, only some of all the 125 basic vectors are chosen, resulting in the current THD increased slightly and the modulation range decreased. The dc-link and FC voltages are controlled by selecting redundant switching states appropriately. The equivalence between carrier-based PWM and SVPWM has also been investigated in many articles [23]–[25]. Complex SVPWM strategies can be equivalently achieved by carrier-based PWM with injecting zero-sequence component [25], [26]. The essential idea is to covert the multilevel converters into two-level converters, and then use the equivalence between two-level SVM and carrier-based PWM. Unfortunately, most of these simplified methods are the special case of equal time distribution between redundant vectors without considering the neutral point voltage and FC voltage balancing problem, which is extremely important for multilevel FC converters like this topology. 5L-FC rectifiers cannot work normally under these simplified strategies. Moreover, some unique strategies with different advantages, such as model predictive control [27], [28], discontinuous PWM [29], selective harmonic elimination PWM [30], and hybrid modulation [31] are also proposed one after another. Essentially, they all achieve the FC and dc-link voltages balance by adjusting the corresponding capacitor currents. There is no doubt that the above strategies can effectively keep the dc-link voltages and FC voltages balanced. However, the NP current caused by basic voltage vectors cannot be fully eliminated in a switching period, resulting in low-frequency NP voltage oscillations.

In order to minimize the low-frequency NP voltage oscillations, large capacity capacitors [32] or extra balancing circuits [33] can be adopted, whereas the system cost and bulk are increased. Solutions based on modulation techniques are more appropriate. In three-level filed, according to the principle that the average NP current in a carrier period should be zero, several modulation methods with unique advantages have been proposed, including adopting virtual vectors [34], [35], injecting optimal compensation value to reference signals [36], adjusting the relative dwell time of basic vectors [37], [38], using double modulation waves [39], adopting hybrid modulation strategies [40], etc. They are effective and instructive. Nevertheless, due to the difference of topological structure, the above strategies cannot be successfully applied to 5L-FC rectifiers.

Based on the above review, there are few effective modulation strategies for mitigating the NP voltage oscillations in the 5L-FC rectifier currently. For addressing this issue, a compensation component injection method based on a hybrid modulation combining the advantages of PDPWM and PSPWM is proposed. Optimal compensation component is injected to make the NP current equal to zero for minimizing the NP voltage oscillations.

TABLE I
SWITCHING STATES OF 5L-FC RECTIFIER WITH EFFECTS ON NP AND FC

i_k	S_{k1}	S_{k2}	V_{kn}	S	i_{kf}	i_{kn}	F
+	1	1	$0.5V_{dc}$	V_1	0	0	4
	1	0	$0.25V_{dc}$	V_2	i_k	i_k	3^+
	0	1	$0.25V_{dc}$	V_3	$-i_k$	0	3^-
	0	0	0	V_4	0	i_k	2_+
-	1	1	0	V_5	0	i_k	2_-
	0	1	$-0.25V_{dc}$	V_6	$-i_k$	i_k	1^+
	1	0	$-0.25V_{dc}$	V_7	i_k	0	1^-
	0	0	$-0.5V_{dc}$	V_8	0	0	0

The rest of this article is organized as follows. In Section II, the operational characteristic of the 5L-FC rectifier is presented. In Section III, a hybrid modulation and its characteristics are detailly presented. Then, a compensation component injection method based on the hybrid modulation is proposed to minimize the NP voltage oscillations. In Section IV, simulations and experiments are presented to verify the performance of the proposed compensation method. Finally, Section V concludes this article.

II. OPERATIONAL CHARACTERISTICS OF 5L-FC RECTIFIER

As shown in Fig. 1, the topology consists of four switches and one FC in each phase leg. The rated voltage of both the upper and lower dc-link capacitor is $0.5V_{\rm dc}$, and three-phase FC voltages should be regulated at $0.25V_{\rm dc}$. i_k and $i_{\rm kn}$ are the phase current and phase NP current, respectively, where k represents phases a, b, and c. (S_{k1}, S'_{k1}) and (S_{k2}, S'_{k2}) are two pairs of complementary switch pairs. In addition, i_{kf} and V_{kf} are the corresponding FC current and voltage. Their positive directions are marked by the red arrows in Fig. 1. The NP is referred as the zero potential.

Each phase leg of the 5L-FC rectifier can produce five voltage levels with eight distinctive switching states $V_1 \sim V_8$, as given in Table I. For convenience, the five voltage levels $-0.5V_{\rm dc}$, $-0.25V_{\rm dc}$, 0, $0.25V_{\rm dc}$, $0.5V_{\rm dc}$ are represented by 0, 1, 2, 3, 4. Note that, $\pm 0.25V_{\rm dc}$ have two redundant switching states (V_2 and V_3, V_6 and V_7), which have opposite effects on the FCs and can be used to regulate the FC voltages. Thus, 1^+ and 3^+ denote that the corresponding switching states charge the FC while 1^- and 3^- denote that the corresponding switching states discharge the FC. It is worth emphasizing that 1^+ and 3^+ also affect the NP potential, as shown in Table I, which means dynamic FC voltage regulation will oscillate the NP voltage. This is the inherent coupling problem between FCs and NP. V_4 and V_5 have the same output voltage level and same effect on FC and NP. They are distinguished by 2_+ and 2_-.

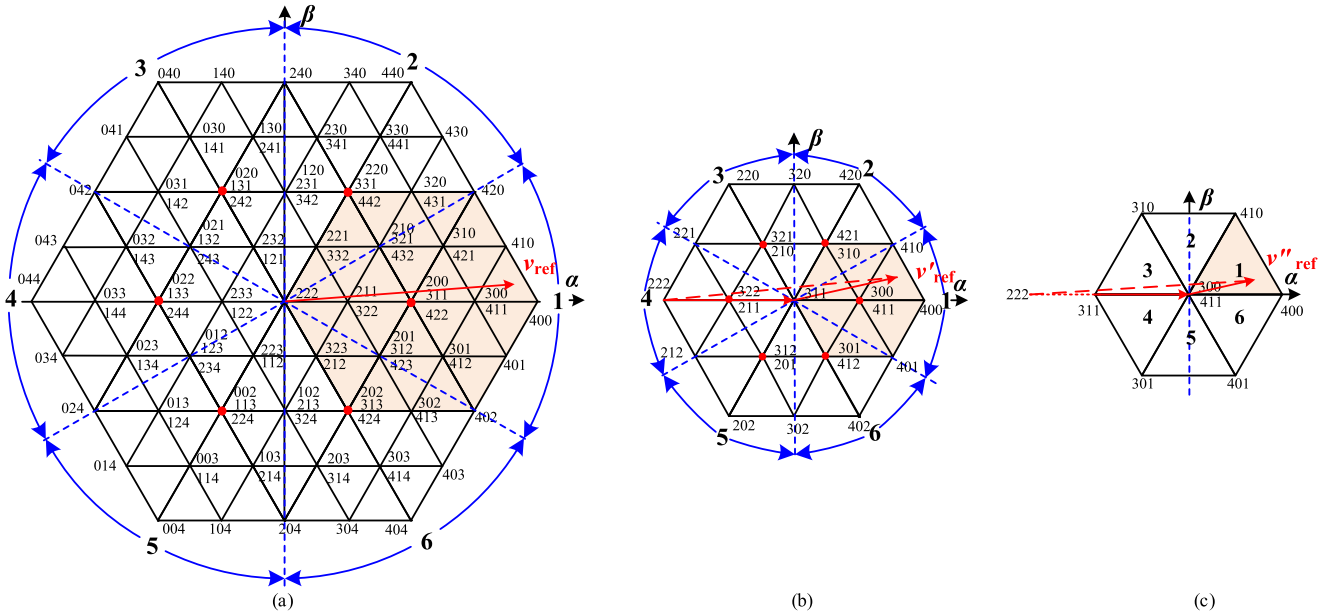

Fig. 2. Space vector diagram. (a) 5L space vector diagram. (b) Modified 3L space vector diagram ($N_3 = 1$). (c) Modified 2L space vector diagram ($N_2 = 1$).

Note that the generated terminal voltage of the rectifier is not only determined by switching states, but also related to the polarity of the phase current, as given in Table I. Thus, to achieve unity power factor at the ac source terminals, there are inevitably current distortions near the zero-crossing points [41]. To solve the problem, unity power factor operation is considered at the rectifier input terminals [42], [43]. Since the proportion of the reactive power required by the filter is small, the power factor at the ac source is still close to unity. This article adopts the current-oriented control strategy proposed in [42] to operate the rectifier.

When the grid is balanced, the input currents i_{k} can be expressed as

$$\begin{cases} i_{\mathrm{a}} = I_{\mathrm{m}} \cos(\theta) \\ i_{\mathrm{b}} = I_{\mathrm{m}} \cos(\theta - 2\pi/3) \\ i_{\mathrm{c}} = I_{\mathrm{m}} \cos(\theta + 2\pi/3) \end{cases} \tag{1}$$

where I_m and θ are the amplitude and phase angle of the input currents, respectively. Thus, three-phase reference signals $v_{\mathrm{k\_ref}}$ can be expressed as

$$\begin{cases} v_{a\_\mathrm{ref}} = m \cos(\theta) \\ v_{b\_\mathrm{ref}} = m \cos(\theta - 2\pi/3) \\ v_{c\_\mathrm{ref}} = m \cos(\theta + 2\pi/3) \end{cases} \tag{2}$$

where m is the modulation index which is normalized at $0.5V_{\mathrm{dc}}$. It satisfies $0 < m < 1.15$.

The instantaneous NP current is the sum of three-phase currents flowing across the NP, which can be expressed as

$$i_n = i_a S_a + i_b S_b + i_c S_c \tag{3}$$

where S_k satisfies

$$S_k = \begin{cases} 1, F = 3^+, 2, 1^+ \\ 0, \text{else}. \end{cases} \tag{4}$$

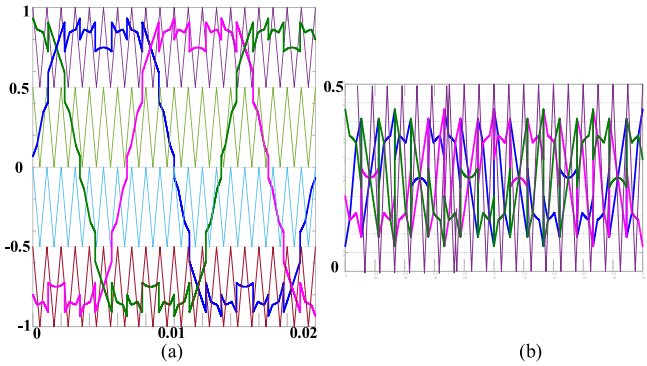

Fig. 3. Reference signal waveforms under the simplified SVM method ($m = 1$). (a) Equivalent reference signals v'_{k_eq}. (b) Modulation wavs m_{k}.

If the average value of the NP current i_{n} in a carrier period can be controlled to zero, the NP voltage oscillations can be effectively mitigated.

III. Proposed Hybrid Modulation and Compensation Component Injection Method

A. Traditional Simplified SVM Method

The equivalence between CBPWM and multilevel SVPWM has been analyzed and proved in many articles [23]–[25]. The essential idea is to transform the complex n-level SVD into simple two-level SVDs by sector divisions and vector corrections, as shown in Fig. 2, and then use the equivalence between two-level SVM and carrier-based PWM. Detailed implementation processes of the simplified SVM method for five-level converters are shown in Appendix.

Fig. 3 shows the reference signal waveforms under the simplified SVM method. By comparing the equivalent reference

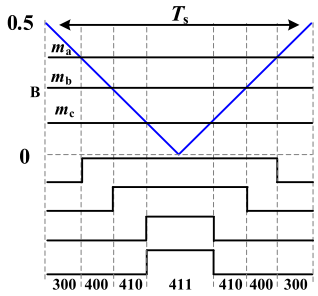

Fig. 4. Switching sequence when $N = 111$.

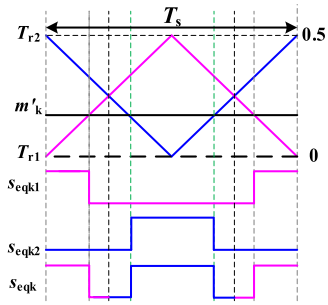

Fig. 5. Implementation diagram of the hybrid modulation.

signals v'_{k_eq} with four symmetrical level-shifted triangular carriers, the seven-segment switching sequence can be obtained, which is composed of nearest three vectors (NTVs).

For convenience, defining N as the total sector label, it can be written as

$$N = 100N_5 + 10N_3 + N_2 \tag{5}$$

where N_5, N_3, and N_2 are the sector labels of the 5L-SVD, 3L-SVD, and 2L-SVD, shown in Fig. 2, respectively.

For the convenience of the following analysis, the equivalent reference signals are further folded between 0 and 0.5 with one triangular carrier, as shown in Fig. 3(b). Define the modulation waves m_k representing the folded reference signals. When $N = 111$, the generated switching sequence is shown in Fig. 4, composed of NTVs including 411(300), 400, and 410.

It is worth emphasizing that, the simplified SVM method considerably simplifies the calculation, but only consider the case of equal time distribution between redundant vectors without the voltage control capability of FC and NP voltages. Thus, this simplified method is not suitable for multilevel FC converters especially 5L-FC rectifiers, resulting in failing to work. For solving these problems, this article proposes a compensation component injection method based on a hybrid modulation, as presented as follows.

B. Proposed Hybrid Modulation

PDPWM is known to have best line voltage harmonic performance, while the conduction and switching losses are not uniformly distributed [18]. On the contrary, PSPWM has the ability of natural FC voltage balancing and simple control while the line voltage harmonic performance is worse [16]. To combine their advantages, this article proposes a hybrid modulation.

The implementation diagram of the proposed hybrid modulation is shown in Fig. 5. The modified modulation wave m'_k is half of the original modulation wave m_k, which can be expressed as

$$m'_k = \frac{1}{2}m_k \tag{6}$$

where m_k is the modulation waves shown in Fig. 3(b).

The phases of carrier waves T_{r1} and T_{r2} are shifted by 180°, identical to PSPWM. Comparing m'_k with T_{r1}, T_{r2}, respectively, switching sequence s_{eqk1} and s_{eqk2} can be obtained. The final switching sequence s_{eqk} is obtained by combining s_{eqk1} and s_{eqk2}, as shown in Fig. 5. It is regulated that 1 and 3 of s_{eqk1} adopt 1^+ and 3^+ while those of s_{eqk2} adopt 1^- and 3^-. In other words, s_{eqk1} charges FC while s_{eqk2} discharges FC.

Fig. 6 shows the contrast waveforms of the proposed hybrid modulation and PSPWM with different ranges of modulation waves. It can be clearly seen that, due to that a pair of redundant switching states are always used in one carrier period, FC voltage keeps same at both the starting and ending of the carrier period. Thus, both two modulation strategies have the ability of natural FC voltage balancing. Note that, when the modulation wave falls in the range of (0.5, 1) and $(-0.5, 0)$, as shown in Fig. 6(b) and (c), the hybrid modulation uses the redundant switching states twice, which is beneficial for reducing the FC voltage ripple amplitude (only half of that of PSPWM) while the switching loss is doubled. In a complete fundamental period, the switching loss of the proposed hybrid modulation is increased by about 50% compared with PSPWM under the condition of same carrier frequency.

Fig. 7 further shows the line voltage waveforms, harmonic spectra and number of switching transitions in a fundamental period under three modulation strategies including the proposed hybrid modulation, PSPWM and PDPWM. They are compared with the same equivalent switching frequency ($f_{\mathrm{PDPWM}} = 2f_{\mathrm{PSPWM}} = 3f_{\mathrm{hybrid\ modulation}}$). To present clearly, the modulation waves are also not folded. In practical applications, the modulation waves can be folded to save carriers and reduce calculations.

It can be clearly seen in Fig. 7(a) that PSPWM synthesizes the average line voltage V_{ab} by using three nearest levels in some zones (red circles in Fig 7(a)), reducing the quality of line voltage (THD = 25.51%). The harmonic components mainly concentrate near twice the carrier frequency. But since a pair of switching states with opposite effects on FC voltage is always used in each carrier period, uniformly distributed conduction and switching losses and natural FC voltage balancing ability are obtained. PDPWM always synthesizes the average line voltage by using two nearest levels to obtain optimal harmonic performance (THD = 17.00%). The main harmonics concentrate around the carrier frequency and twice the carrier frequency, as shown in Fig. 7(b). However, it lacks natural FC voltage balancing ability. Conduction and switching losses are distributed nonuniformly.

The proposed hybrid modulation can be viewed as a combination of PSPWM and PDPWM. Fig. 7(c) shows the characteristics of the proposed hybrid modulation. It can be clearly

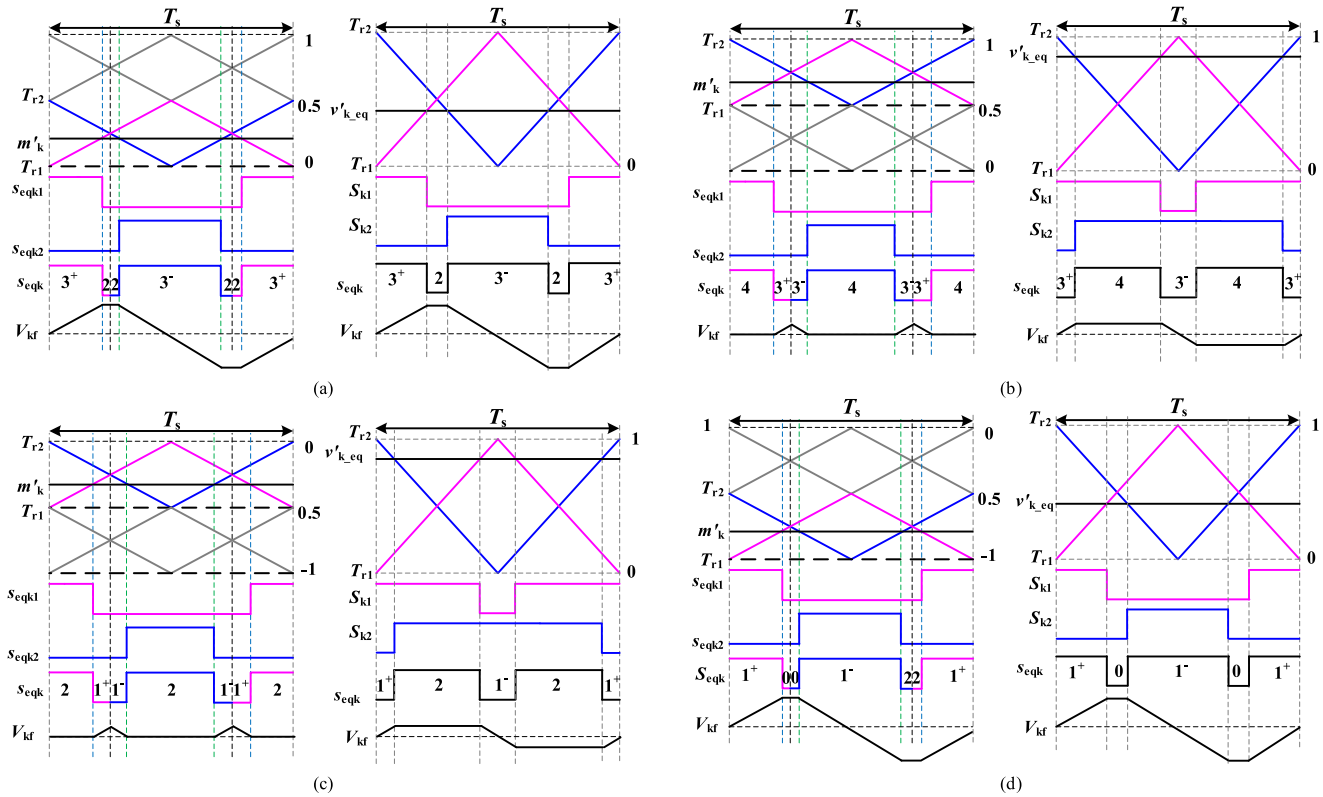

Fig. 6. Modulation diagram under proposed hybrid modulation (left) and PSPWM (right) with different ranges of modulation waves. (a) $0 < v'_{k\_eq} < 0.5$. (b) $0.5 < v'_{k\_eq} < 1$. (c) $-0.5 < v'_{k\_eq} < 0$. (d) $-1 < v'_{k\_eq} < -0.5$.

seen that the hybrid modulation also synthesizes the average line voltage by using two nearest levels, so it has the same optimal harmonic characteristic as PDPWM (THD = 17.06%). The harmonic components are mainly around four times the carrier frequency, which can be easily filtered out by filters. A pair of redundant switching states is used in one carrier period, resulting in the same natural voltage balancing ability for FC as PSPWM. Meanwhile, the conduction and switching losses are distributed evenly, which is good for heat sink design.

C. Injecting Optimized Compensation Component for NP Voltage Oscillations Minimization

Adopting the hybrid modulation, the generated three-phase switching sequence is shown in Fig. 8 and Fig. 9, which is redistributed for obtaining natural FC voltage balancing ability compared with the sequence shown in Fig. 4. The 7-segment switching sequence becomes 15-segment switching sequence. For mitigating the NP voltage oscillations, the average NP current in a carrier period should be zero. Injecting optimal compensation component can help achieve this aim. The modulation waves after injecting compensation component m''_k are expressed as

$$m''_k = m'_k + m_{\rm ac} \tag{7}$$

where $m_{\rm ac}$ is the optimized compensation component to compensate the average NP current.

1) When N = 111∼116, the redundant vectors are 300/411.

According to Table I, only when the output voltage is 3^+, 2 and 1^+ are there currents flowing across the NP. After injecting $m_{\rm ac}$, the average NP current in a carrier period $i_{\rm n\_ave}$ is set to zero, which is expressed as

$$\begin{aligned} i_{n\_\rm ave} &= \sum_{\rm k}^{k=a,b,c} (t_{k3^+} + t_{k2} + t_{k1^+}) \cdot i_k \\ &= t_{a3^+} i_a + t_{b1^+} i_b + t_{c1^+} i_c = 0 \end{aligned} \tag{8}$$

where t_{k3+}, t_{k2}, t_{k1+} is the dwell time of 3^+, 2, 1^+ in a carrier period, respectively. t_{a3+}, t_{b1+}, t_{c1+} can be expressed as

$$\begin{cases} t_{a3^+} = 0.25 - 0.5 m_a \\ t_{b1^+} = 0.5 m_b \\ t_{c1^+} = 0.5 m_c. \end{cases} \tag{9}$$

Combining (8) and (9), $m_{\rm ac}$ can be solved as

$$m_{\rm ac} = (\Delta_1 + 0.25\Delta_2)/i_a \tag{10}$$

where Δ_1 and Δ_2 are expressed as

$$\begin{cases} \Delta_1 = 0.125 i_a \\ \Delta_2 = -m_a i_a + m_b i_b + m_c i_c. \end{cases} \tag{11}$$

2) For N = 211∼216, the redundant vectors involved in synthesizing the reference vector are 320/431. $i_{\rm n\_ave}$ is set to

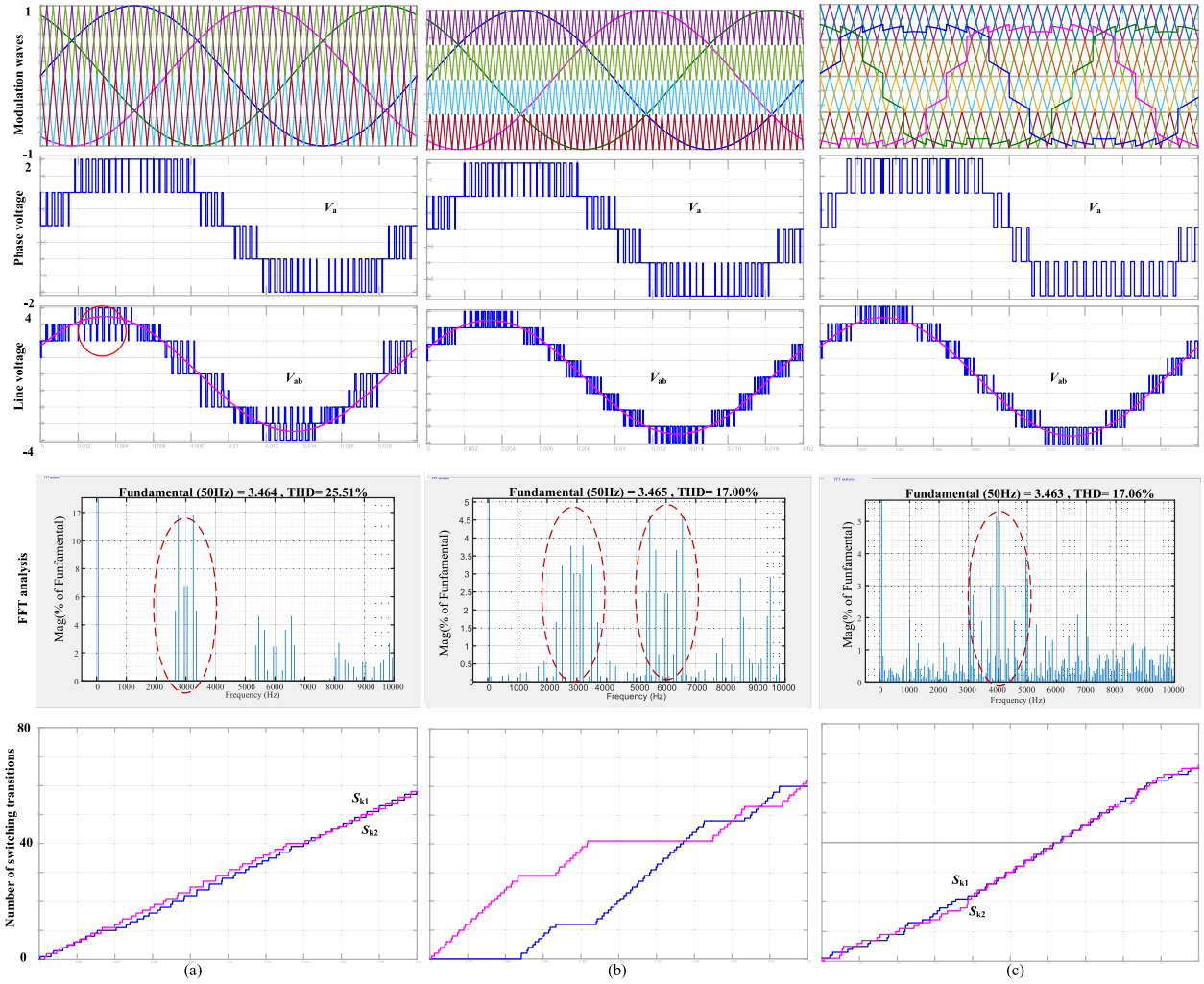

Fig. 7. Line voltage waveforms, harmonic spectra and number of switching transitions in a fundamental period under three modulation strategies (carrier frequency: $f_{\mathrm{PDPWM}} = 2f_{\mathrm{PSPWM}} = 3f_{\mathrm{hybrid\ modulation}}$) fundamental frequency: 50 Hz, modulation index: $m = 1$). (a) PSPWM (1.5 kHz). (b) PDPWM (3 kHz). (c) Proposed hybrid modulation (1 kHz).

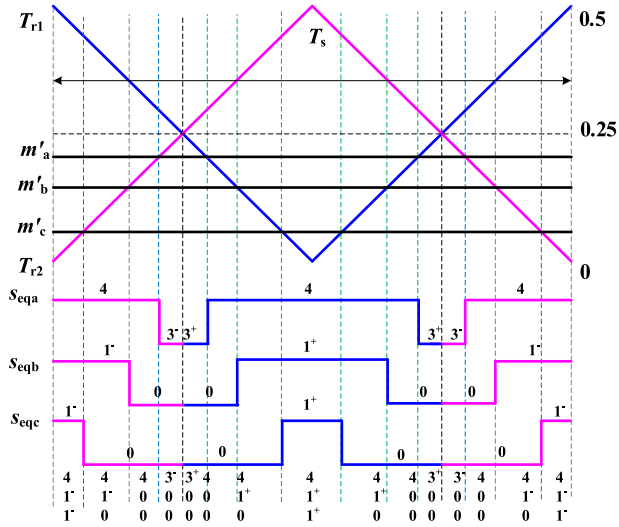

Fig. 8. 15-segment switching sequence when $N = 111$.

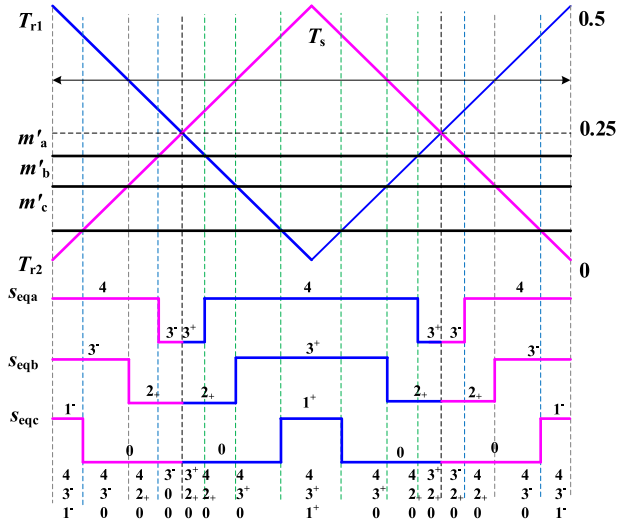

Fig. 9. 15-segment switching sequence when $N = 211$.

TABLE II
OPTIMAL COMPENSATION COMPONENT IN DIFFERENT SECTORS

N_S	N_3	Δ_1, Δ_2	m_{ac}	N_S	N_3	Δ_1, Δ_2	m_{ac}
1	1	$\Delta_1=0.125i_a$	$\begin{cases}\Delta_2=-m_ai_a+m_bi_b+m_ci_c\\ m_{ac}=\dfrac{\Delta_1+0.25\Delta_2}{i_a}\end{cases}$	4	1	$\Delta_1=-0.125i_a$	$\begin{cases}\Delta_2=m_ai_a-m_bi_b-m_ci_c\\ m_{ac}=\dfrac{-(\Delta_1+0.25\Delta_2)}{i_a}\end{cases}$
	2	$\Delta_1=-0.125i_c$			2	$\Delta_1=0.125i_c$	
	3	$\Delta_1=0.25i_a+0.125i_b$			3	$\Delta_1=0.125i_b+0.25i_c$	
	4	$\Delta_1=0.125i_a$			4	$\Delta_1=-0.125i_a$	
	5	$\Delta_1=0.25i_a+0.125i_c$			5	$\Delta_1=0.25i_b+0.125i_c$	
	6	$\Delta_1=-0.125i_b$			6	$\Delta_1=0.125i_b$	
2	1	$\Delta_1=0.125i_a+0.25i_b$	$\begin{cases}\Delta_2=-m_ai_a-m_bi_b+m_ci_c\\ m_{ac}=\dfrac{-(\Delta_1+0.25\Delta_2)}{i_c}\end{cases}$	5	1	$\Delta_1=0.125i_a+0.25i_c$	$\begin{cases}\Delta_2=m_ai_a+m_bi_b-m_ci_c\\ m_{ac}=\dfrac{\Delta_1+0.25\Delta_2}{i_c}\end{cases}$
	2	$\Delta_1=-0.125i_c$			2	$\Delta_1=0.125i_c$	
	3	$\Delta_1=0.25i_a+0.125i_b$			3	$\Delta_1=0.125i_b+0.25i_c$	
	4	$\Delta_1=0.125i_a$			4	$\Delta_1=-0.125i_a$	
	5	$\Delta_1=-0.125i_c$			5	$\Delta_1=0.125i_c$	
	6	$\Delta_1=0.125i_b$			6	$\Delta_1=-0.125i_b$	
3	1	$\Delta_1=0.125i_a+0.25i_b$	$\begin{cases}\Delta_2=m_ai_a-m_bi_b+m_ci_c\\ m_{ac}=\dfrac{(\Delta_1+0.25\Delta_2)}{i_b}\end{cases}$	6	1	$\Delta_1=0.125i_a+0.25i_c$	$\begin{cases}\Delta_2=-m_ai_a+m_bi_b-m_ci_c\\ m_{ac}=\dfrac{-(\Delta_1+0.25\Delta_2)}{i_b}\end{cases}$
	2	$\Delta_1=-0.125i_c$			2	$\Delta_1=0.125i_c$	
	3	$\Delta_1=0.125i_b$			3	$\Delta_1=-0.125i_b$	
	4	$\Delta_1=-0.125i_a$			4	$\Delta_1=0.125i_a$	
	5	$\Delta_1=0.25i_b+0.125i_c$			5	$\Delta_1=0.25i_a+0.125i_c$	
	6	$\Delta_1=0.125i_b$			6	$\Delta_1=-0.125i_b$	

zero, which can be written as

$$i_{n\_ave}=t_{a3+}i_a+(t_{b2}+t_{b3+})i_b+t_{c1+}i_c=0. \tag{12}$$

Fig. 9 shows the corresponding switching sequence when $N=211$. The dwell time t_{a3+}, t_{b2}, t_{b3+}, t_{c1+} can be expressed as

$$\begin{cases}t_{a3+}=0.25-0.5m_a, t_{b2}=0.5-m_b\\ t_{b3+}=0.5m_b, t_{c1+}=0.5m_c.\end{cases} \tag{13}$$

Combining (12) and (13), m_{ac} can be solved as

$$m_{ac}=-(\Delta_1+0.25\Delta_2)/i_c \tag{14}$$

where Δ_1 and Δ_2 are expressed as

$$\begin{cases}\Delta_1=0.125i_a+0.25i_b\\ \Delta_2=-m_ai_a-m_bi_b+m_ci_c.\end{cases} \tag{15}$$

The 5L-SVD can be divided into 36 2L-SVDs, so there are 36 cases in total. They are solved and given in Table II.

It should be noted that the compensation component m_{ac} only makes the average NP current equal to zero for mitigating the low-frequency NP voltage oscillations in balanced cases. But, if the initial dc-link voltages are unbalanced, this unbalanced voltage will be reserved. To effectively solve this problem, dc compensation component also needs to be injected. It is related to the voltage error (V_2-V_1) and can be simply expressed as

$$m_{dc}=\frac{V_2-V_1}{V_{dc}}. \tag{16}$$

Define m_o as the total compensation component. It is expressed as

$$m_o=m_{ac}+m_{dc}. \tag{17}$$

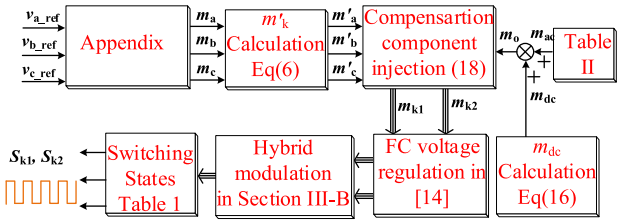

Fig. 10. Control diagram of the proposed compensation method based on the hybrid modulation.

Correspondingly, (7) is modified as

$$m_k''=m_k'+m_o \tag{18}$$

where m_k'' satisfies $0<m_k''<0.25$.

D. Control Diagram of the Proposed Compensation Method

Based on the above analysis, the overall control diagram of the proposed compensation method based on the hybrid modulation is presented in Fig. 10. It can be divided into five steps as follows.

1) *Equivalent Reference Signals Calculation:* Traditional 5L-SVPWM strategies are too complex. For reducing the calculations, an existing simplified SVM method is adopted to calculate the equivalent reference signals, which greatly simplifies the calculations. Detailed process is shown in the Appendix.
2) *NP Voltage Minimization:* For minimizing the NP voltage oscillations, optimal compensation component is simultaneously injected to the modulation waves. The complex

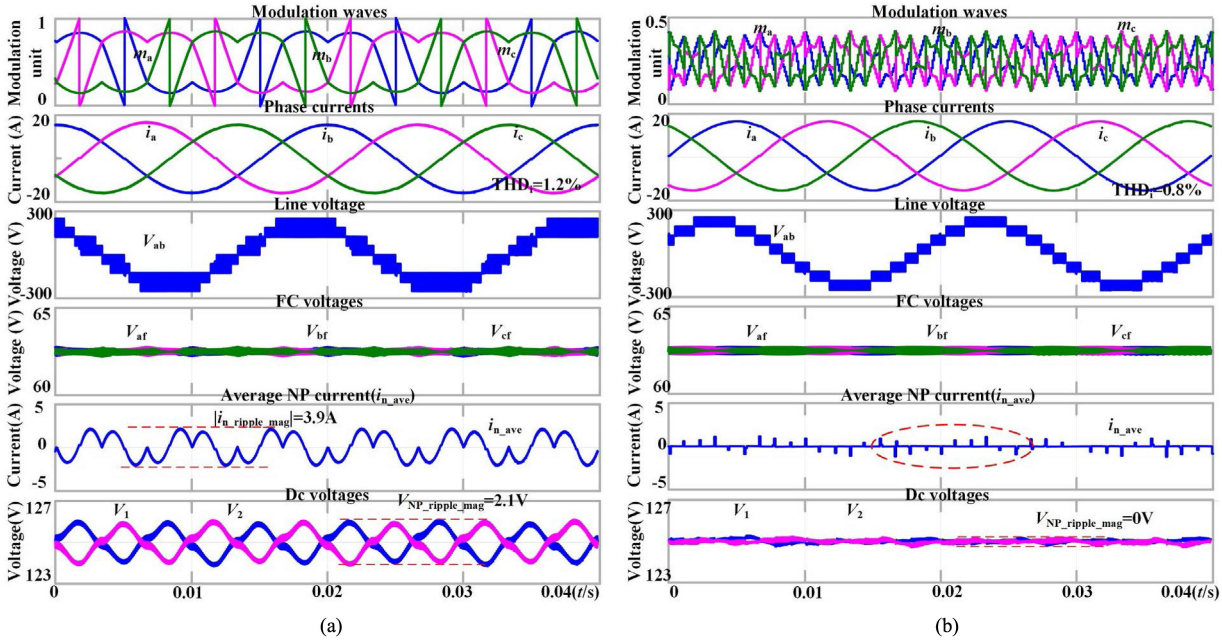

Fig. 11. Simulation waveforms with case 1. (a) Conventional PSPWM. (b) Proposed hybrid modulation.

5L-SVD can be divided into 36 2L-SVDs. Thus, there are 36 cases in total given in Table II.

3) *FC Voltage Regulation:* The hybrid modulation is essentially a modification of PSPWM. Thus, under ideal situations, the FC voltages are naturally balanced without any voltage feedback control. To enhance the voltage balancing performance, they can be regulated by adjusting the modulation waves of S_{k1}, S_{k2}, similar to PSPWM. Detailed process is shown in [14].
4) *Hybrid Modulation:* For combining the same superior harmonic performance as PDPWM and the same natural voltage balancing ability as PSPWM, a hybrid modulation is proposed.
5) *Switching States Generation:* Comparing the generated switching sequence s_{eqk} with Table I, the switching states of S_{k1} and S_{k2} can be obtained to control the rectifier.

IV. Simulations and Experimental Results

To verify the performance of the proposed compensation method based on the hybrid modulation, both simulations and experiments were carried out to compare with PSPWM. The parameters of the simulations and experiments are given in Table III. Two cases are considered as follows.

1) *Case* 1 *($m \approx 1$):* The line voltage V_{ab}(rms) is kept at 150 V. The total dc voltage is regulated at 250 V with a resistive load $R = 21\ \Omega$.
2) *Case* 2 *($m \approx 0.65$):* The line voltage V_{ab}(rms) is kept at 100 V. The total dc voltage is regulated 250 V with a resistive load $R = 34\ \Omega$.

A. Simulation Results Analysis

Fig. 11 shows the waveforms of modulation waves, phase currents, line voltage, FC voltages, two dc voltages and average NP current under the conditions of case 1. Three-phase FC voltages are regulated at 62.5 V ($0.25V_{\mathrm{dc}}$). Conventional PSPWM is applied in Fig. 11(a) ($\mathrm{THD_i} = 1.2\%$). This method generates the average line voltage V_{ab} by using three nearest levels, resulting in poor line voltage harmonic performance, as described in Section II-B. Meanwhile, due to the influence of the NP current, there are obvious low-frequency voltage oscillations at the NP. The frequency of the average NP current i_{n_ave} is three times the fundamental frequency, and its magnitude $i_{n\_\mathrm{ripple\_mag}}$ reaches 3.9 A, causing the magnitude of NP voltage oscillations $V_{\mathrm{NP\_ripple\_mag}}$ to reach 2.1 V. Comparatively, Fig. 11(b) adopts the proposed hybrid modulation. ($\mathrm{THD}_i = 0.8\%$). The line voltage V_{ab} behaves as a typical nine-level waveform. Better harmonic performance is obtained compared with PSPWM. With injecting compensation component m_{ac}, $i_{n\_\mathrm{ripple\_mag}}$ is close to zero, resulting in $\mathrm{V_{NP\_ripple\_mag}}$ approximately equal to 0 V. Note that, there are still some small intervals where i_{n_ave} is not equal to zero. That is because the solved compensation component cannot fully compensate the NP current caused by

TABLE III
Parameters of Simulations and Experiments

Parameters	Values
Input line voltage (rms) e_{k}	100/150V(50Hz)
DC-link voltage V_{dc}	250V
DC-link capacitor C_1/C_2	1200μF
FC voltage V_{kf}	62.5V
FC	560μF
L-filter	1.5mH
Frequency	10kHz
DC load R	21/34Ω

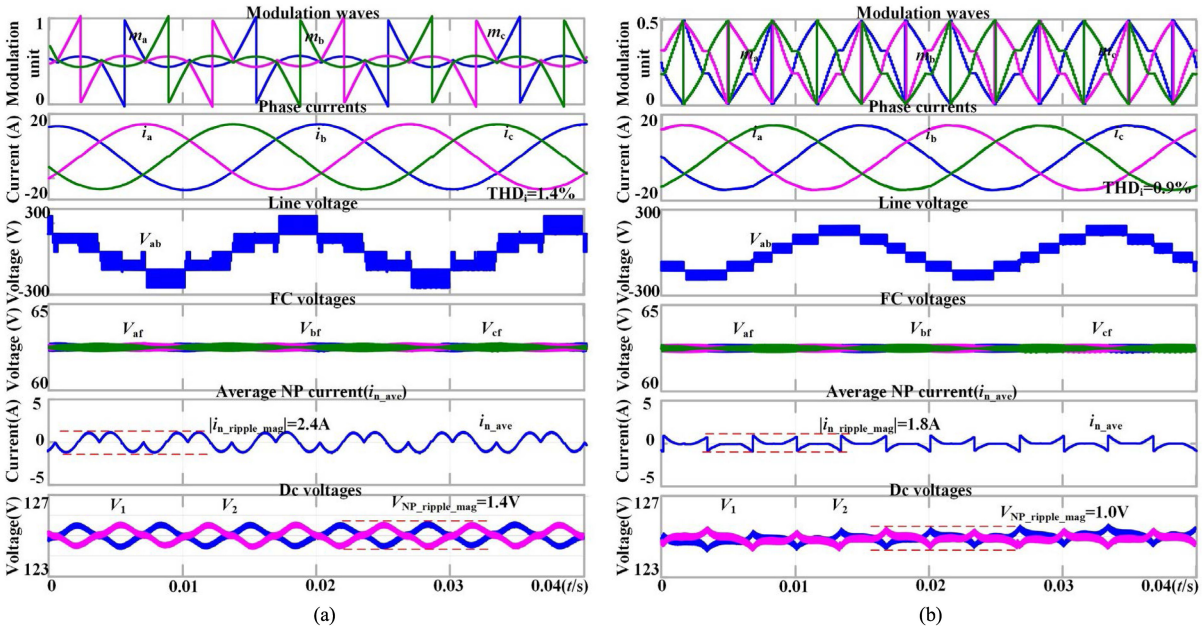

Fig. 12. Simulation waveforms under case 2. (a) Conventional PSPWM. (b) Proposed hybrid modulation.

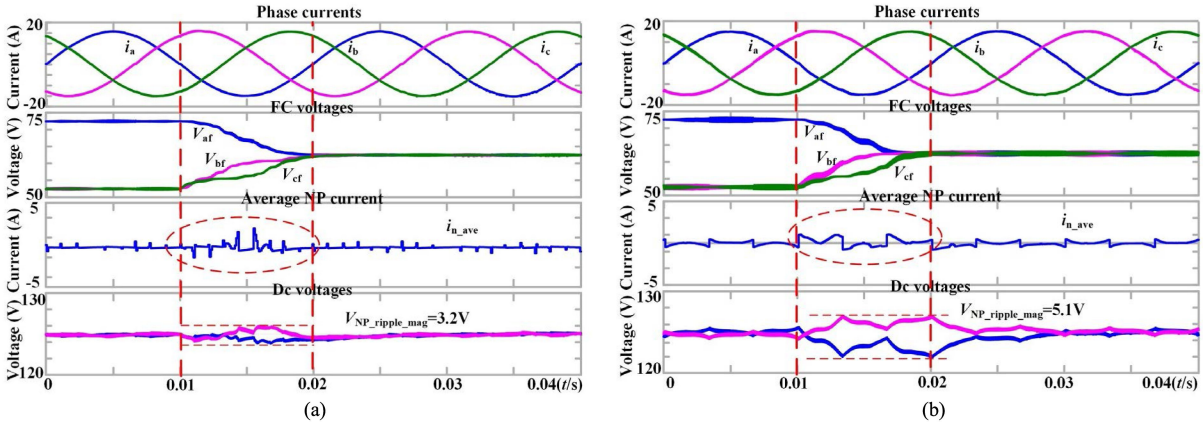

Fig. 13. Simulation waveforms of FC voltage control with the proposed hybrid modulation. (a) Case 1. (b) Case 2.

1^+, 2, and 3^+ due to the limited range of modulation waves. Since the proportion of these intervals is very small, they can be ignored. Simulations strongly verify the effectiveness and performance of the proposed method.

Fig. 12 shows the comparative waveforms in case 2. Fig. 12(a) adopts the conventional PSPWM (THD$_i$ = 1.4%). $i_{n\_ripple\_mag}$ is 2.4 A, resulting in $V_{NP\_ripple\_mag}$ reaching 1.4V. Fig. 12(b) adopts the proposed hybrid modulation. Better line current quality is obtained. (THD$_i$ = 0.9%). V_{ab} behaves as a seven-level waveform. $i_{n\_ripple\_mag}$ reaches 1.8 A, smaller than that of PSPWM. Correspondingly, $V_{NP\_ripple\_mag}$ is reduced to 1.0V. Due to the range limitation of modulation waves, there are also some intervals where i_{n_ave} does not equal zero but i_{n_ave} is minimized. Comparing Fig. 11(a) and (b), it can be found that the NP voltage oscillations mitigation effect of the proposed compensation method is related to the modulation index. the higher the modulation index is, the better the mitigation effect performs.

Fig. 13 further verifies the performance of dynamic FC voltage regulation with the proposed hybrid modulation in these two cases. Initially, three-phase FC voltages are regulated at 75, 50 and 50 V, respectively. At 0.05 s, they are set to 62.5 V. It can be clearly seen that, in the process of voltage control, $i_{n\_ripple\_mag}$ increases with resulting in $V_{NP\_ripple\_mag}$ increasing. The injected compensation component cannot fully compensate the NP current caused by 1^+, 2, and 3^+, but the average NP current is minimized. The maximum value of $V_{NP\_ripple\_mag}$ only reaches 3.2 and 5.1 V, which is completely acceptable. In steady state, $i_{n\_ripple\_mag}$ is approximately equal to zero, effectively minimizing the NP voltage oscillations.

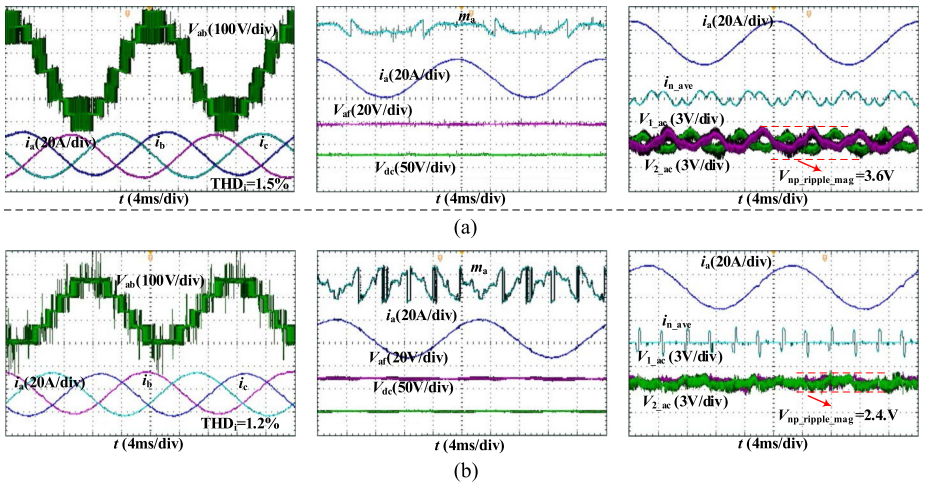

Fig. 14. Experimental waveforms under case 1. (a) Conventional PSPWM method. (b) Proposed hybrid modulation.

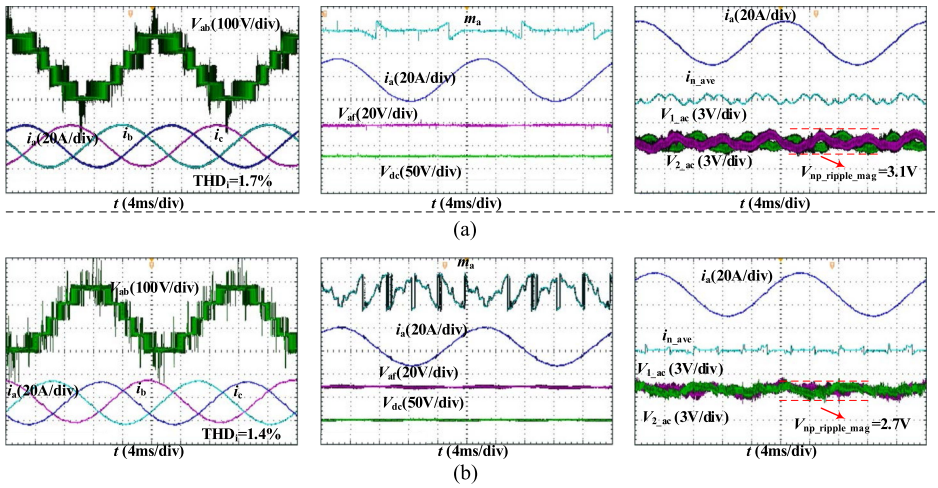

Fig. 15. Experimental waveforms under case 2. (a) Conventional PSPWM method. (b) Proposed hybrid modulation.

B. Experimental Results Analysis

To further verify the feasibility and performance of the proposed scheme, experiments were performed in a prototype of 5L-FC rectifier shown in Fig. 17. The experimental parameters are consistent with the simulation parameters given in Table III. The control system of the experimental platform adopts digital signal processing (DSP, TMS320F28337D) and field programmable gate array (FPGA, 10M16SAE144). DSP is used for data processing, and pulse distributions are down by FPGA.

Fig. 14 shows the experimental waveforms including line voltage, phase currents, modulation wave, average NP current, FC voltage and dc voltages in case 1. Note that, phase A modulation wave m_a and average NP current i_{n_ave} are observed by the digital-to-analog converters of DSP. The ac components of two dc voltages V_{1_ac} and V_{2_ac} are measured by selecting ac mode of the oscilloscope. With adopting the current-oriented control strategy, there are no obvious current distortions near the zero-crossing points. The conventional PSPWM is applied in Fig. 14(a)(THD$_i$ = 1.5%). It can be clearly seen that, due to the influence of the average NP current, it exists low- frequency voltage oscillations at the NP with $V_{\mathrm{NP\_ripple\_mag}}$ reaching 3.6 V. Fig. 14(b) adopts the proposed hybrid modulation. The line voltage current quality is improved (THD$_i$ = 1.2%). Phase A FC voltage and the dc-link are balanced in steady state. The line voltage behaves as a typical nine-level waveform, whose harmonic performance is obviously better than that of the conventional PSPWM shown in Fig. 14(a). After injecting m_{ac}, i_{n_ave} in most intervals are mitigated to zero, which results in $V_{\mathrm{NP\_ripple\_mag}}$ decreasing to 2.4 V.

Fig. 15 is the corresponding waveforms under the conditions of case 2. Fig. 15(a) adopts the conventional PSPWM (THD$_i$ = 1.7%). $V_{\mathrm{NP\_ripple\_mag}}$ reaches 3.1 V due to the influence of the average NP current. Comparatively, the proposed hybrid modulation is applied in Fig. 15(b). Better current quality is obtained (THD$_i$ = 1.4%). Furthermore, the injection of m_{ac} reduces the rms value and magnitude of i_{n_ave}, resulting in $V_{\mathrm{NP\_ripple\_mag}}$ reduce to 2.7V. Comparing Figs. 14(b) and 15(b), the same conclusion as that of the simulations can be drawn: the NP voltage oscillations mitigation effect is related

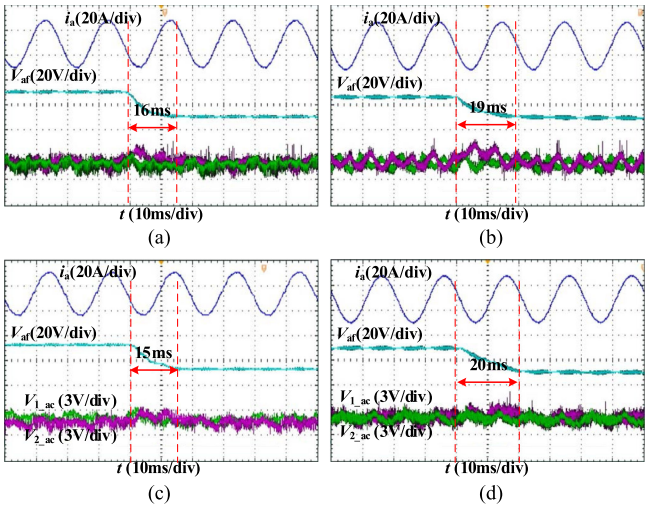

Fig. 16. Experimental waveforms of dynamic FC voltage regulation under PSPWM and the proposed hybrid modulation ($V_{\rm af}$: 80 V→62.5 V). PSPWM: (a) case 1 and (b) case 2. Proposed hybrid modulation: (c) case 1 and (d) case 2.

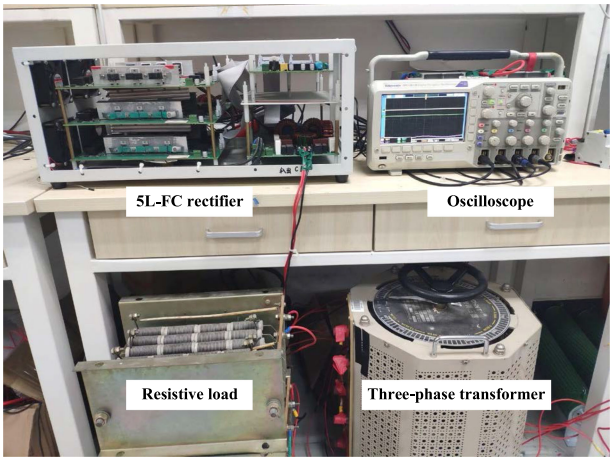

Fig. 17. Schematic diagram of the experimental platform.

to the modulation index. Experimental results also verify the effectiveness and performance of the proposed compensation method based on the hybrid modulation.

Fig. 16 shows the waveforms of dynamic FC voltage regulation in the above two cases. Initially, phase A FC voltage is regulated at 80 V. And then it is set to 62.5 V. As shown in Fig. 16, both modulation strategies can easily control FC voltages by adjusting the relative time of redundant switching states. And there are no obvious voltage oscillations on the two dc voltages during the voltage control process.

Fig. 18 shows the current THD comparisons of the proposed hybrid modulation and PSPWM under different output power and modulation indexes. It can be clearly observed that the proposed hybrid modulation produces better current quality (less THD values) compared with PSPWM, which is consistent with the pervious theoretical analysis.

Table IV and Fig. 19 further present the efficiency comparison and the infrared pictures. Under the same carrier frequency, the switching loss of the proposed hybrid modulation is about 50% higher than that of PSPWM. Hence the efficiency is reduced a little bit. The top temperatures under the proposed hybrid modulation are also a little higher than those under PSPWM.

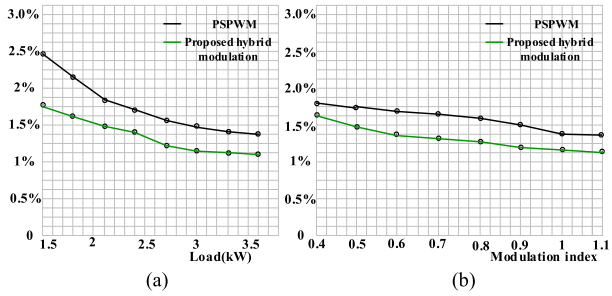

Fig. 18. Current THD comparisons under different output power and modulation indexes. (a) Comparison with different output power ($V_{ab} = 150$ V(rms), $V_{\rm dc} = 250$ V). (b) Comparison with different modulation index [$V_{ab} = 100$ V(rms) and $I_k = 12$ A(rms)].

TABLE IV
COMPARISON OF EFFICIENCY AND TOP TEMPERATURE UNDER TWO MODULATION SCHEMES

Efficiency/Top temperature in the infrared pictures	case 1	case 2
PSPWM	92.66% (64℃)	94.3%(79.3℃)
Proposed hybrid modulation	92.32%(64.3℃)	94.05%(79.6℃)

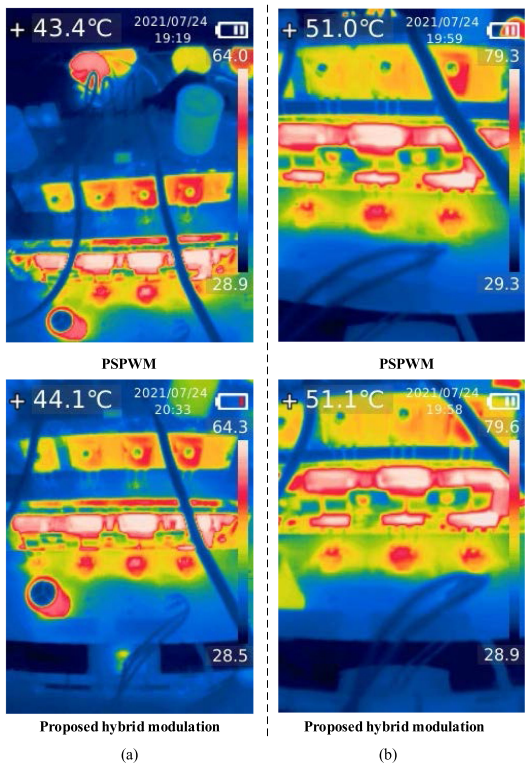

Fig. 19. Infrared pictures under two modulation schemes. (a) Case 1. (b) Case 2.

TABLE V
REFERENCE VOLTAGE CORRECTION OF 3L SVD

N_5	$v'_{\text{a\_ref}}$=	$v'_{\text{b\_ref}}$=
1	$v_{\text{a\_ref}}$-2/3	$v_{\text{b\_ref}}$+1/3
2	$v_{\text{a\_ref}}$-1/3	$v_{\text{b\_ref}}$-1/3
3	$v_{\text{a\_ref}}$+1/3	$v_{\text{b\_ref}}$-2/3
4	$v_{\text{a\_ref}}$+2/3	$v_{\text{b\_ref}}$-1/3
5	$v_{\text{a\_ref}}$+1/3	$v_{\text{b\_ref}}$+1/3
6	$v_{\text{a\_ref}}$-1/3	$v_{\text{b\_ref}}$+2/3

$v'_{c\_\text{ref}} = -v'_{a\_\text{ref}} - v'_{b\_\text{ref}}$.

TABLE VI
REFERENCE VOLTAGE CORRECTION OF 2L SVD

N_3	$v''_{\text{a\_ref}}$=	$v''_{\text{b\_ref}}$=
1	$v'_{\text{a\_ref}}$-1/3	$v'_{\text{b\_ref}}$+1/6
2	$v'_{\text{a\_ref}}$-1/6	$v'_{\text{b\_ref}}$-1/6
3	$v'_{\text{a\_ref}}$+1/6	$v'_{\text{b\_ref}}$-1/3
4	$v'_{\text{a\_ref}}$+1/3	$v'_{\text{b\_ref}}$-1/6
5	$v'_{\text{a\_ref}}$+1/6	$v'_{\text{b\_ref}}$+1/6
6	$v'_{\text{a\_ref}}$-1/6	$v'_{\text{b\_ref}}$+1/3

$v''_{c\_\text{ref}} = -v''_{a\_\text{ref}} - v''_{b\_\text{ref}}$

V. CONCLUSION

To improve the harmonic performance and minimize the NP voltage oscillations in the 5L-FC rectifiers, this article proposes a compensation component injection method based on a hybrid modulation. The hybrid modulation is essentially a combination of PSPWM and PDPWM, hence the advantages of both them are inherited, such as optimal harmonic performance, natural FC voltage balancing ability, even conduction and switching losses, etc. And after injecting optimal compensation component within each subsector of the SVD, the NP current in a carrier period is minimized, which considerably mitigates the NP voltage oscillations. The mitigation effect is related to the modulation index. The higher the modulation index is, the better the mitigation effect performs.

APPENDIX

This appendix shows the implementation steps of the simplified 5L-SVM method. The 5L-SVD can be thought to be composed of six 3L-SVDs, as shown in Fig. 2. Correspondingly, the modified reference voltage vector v_{ref} is equal to the original reference voltage vector v'_{ref} minus the center voltage vector of the selected 3L-SVD (red dots in Fig. 2(a)), as shown in Table V. In the same way, the 3L-SVD can be further divided into six 2L-SVDs. The remodified reference voltage vector v''_{ref} is equal to v'_{ref} minus the center voltage vector of the selected 2L-SVD [red dots in Fig. 2(b)], as given in Table VI. Through the above two steps, the complex 5L-SVD is transformed into simple 2L-SVD.

The 2L-SVPWM can be equivalently achieved by carrier-based PWM with injecting zero-sequence component v_0. It is expressed as

$$v_{\text{o}} = -\frac{v_{\max} + v_{\min}}{2} \tag{19}$$

where $v_{\max}$ and $v_{\min}$ are defined as

$$\begin{cases} v_{\max} = \max\{v''_{a\_\text{ref}}, v''_{b\_\text{ref}}, v''_{c\_\text{ref}}\} \\ v_{\min} = \min\{v''_{a\_\text{ref}}, v''_{b\_\text{ref}}, v''_{c\_\text{ref}}\}. \end{cases} \tag{20}$$

Thus, the final modulation wave m_k is expressed as

$$m_k = v''_{k\_\text{ref}} + v_{\text{o}} + 0.25. \tag{21}$$

Fig. 3(b) shows the corresponding waveform of m_k.

REFERENCES

[1] J.-S. Lee and K.-B. Lee, "A novel carrier-based PWM method for vienna rectifier with a variable power factor," *IEEE Trans. Ind. Electron.,* vol. 63, no. 1, pp. 3–12, Jan. 2016.

[2] A. Rajaei, M. Mohamadian, and A. Y. Varjani, "Vienna-rectifier-based direct torque control of PMSG for wind energy application," *IEEE Trans. Ind. Electron.,* vol. 60, no. 7, pp. 2919–2929, Jul. 2013.

[3] J.-S. Lee and K.-B. Lee, "Predictive control of vienna rectifiers for PMSG systems," *IEEE Trans. Ind. Electron.,* vol. 64, no. 4, pp. 2580–2591, Apr. 2017.

[4] D. F. Cortez and I. Barbi, "A three-phase multilevel hybrid switched-capacitor PWM PFC rectifier for high-voltage-gain applications," *IEEE Trans. Power Electron.,* vol. 31, no. 5, pp. 3495–3505, May 2016.

[5] M. S. Ortmann, S. A. Mussa, and M. L. Heldwein, "Three-phase multilevel PFC rectifier based on multistate switching cells," *IEEE Trans. Power Electron.,* vol. 30, no. 4, pp. 1843–1854, Apr. 2015.

[6] D. Floricau and C. Vlad, "A new five-level rectifier based on parallel switching cells and stacked coupled inductors," in *Proc. Int. Conf. Optim. Elect. Electron. Equip.*, 2014, pp. 621–626.

[7] J.- Itoh, Y. Noge, and T. Adachi, "A novel five-level three-phase PWM rectifier with reduced switch count," *IEEE Trans. Power Electron.,* vol. 26, no. 8, pp. 2221–2228, Aug. 2011.

[8] M. Ke, R. S. Munoz-Aguilar, P. Rodriguez, and F. Blaabjerg, "Thermal and efficiency analysis of five-level multilevel-clamped multilevel converter considering grid codes," *IEEE Trans. Ind. Appl.,* vol. 50, no. 1, pp. 415–423, Jan./Feb. 2014.

[9] M. Narimani, B. Wu, and N. R. Zargari, "A novel five-level voltage source inverter with sinusoidal pulse width modulator for medium-voltage applications," *IEEE Trans. Power Electron.,* vol. 31, no. 3, pp. 1959–1967, Mar. 2016.

[10] G. H. P. Ooi, A. I. Maswood, and Z. Lim, "Five-level multiple-pole PWM AC–AC converters with reduced components count," *IEEE Trans. Ind. Electron.,* vol. 62, no. 8, pp. 4739–4748, Aug. 2015.

[11] D. Mukherjee and D. Kastha, "A reduced switch hybrid multilevel unidirectional rectifier," *IEEE Trans. Power Electron.,* vol. 34, no. 3, pp. 2070–2081, Mar. 2019.

[12] D. Mukherjee and D. Kastha, "A minimum switch five-level unidirectional rectifier without any voltage balancing and pre-charging circuitry," *IEEE Trans. Power Electron.,* vol. 34, no. 12, pp. 11605–11615, Dec. 2019.

[13] D. Floricau and V. Pangratie, "New unidirectional five-level VIENNA rectifier for high-current applications," in *Proc. 39th Ann. Conf. IEEE Ind. Electron. Soc.*, 2013, pp. 1080–1085.

[14] K. Wang, L. Xu, Z. Zheng, and Y. Li, "Capacitor voltage balancing of a five-level ANPC converter using phase-shifted PWM," *IEEE Trans. Power Electron.,* vol. 30, no. 3, pp. 1147–1156, Mar. 2015.

[15] K. Wang, Z. Zheng, Y. Li, K. Liu, and J. Shang, "Neutral-point potential balancing of a five-level active neutral-point-clamped inverter," *IEEE Trans. Ind. Electron.,* vol. 60, no. 5, pp. 1907–1918, May 2013.

[16] K. Wang, Z. Zheng, B. Fan, L. Xu, and Y. Li, "A modified PSPWM for a five-level hybrid-clamped inverter to reduce flying capacitor size," *IEEE Trans. Ind. Appl.,* vol. 55, no. 2, pp. 1658–1666, Mar./Apr. 2019.

[17] A. M. Y. M. Ghias, J. Pou, G. J. Capella, P. Acuna, and V. G. Agelidis, "On improving phase-shifted PWM for flying capacitor multilevel converters," *IEEE Trans. Power Electron.,* vol. 31, no. 8, pp. 5384–5388, Aug. 2016.

[18] K. Wang, Z. Zheng, L. Xu, and Y. Li, "An optimized carrier-based PWM method and voltage balancing control for five-level ANPC converters," *IEEE Trans. Ind. Electron.,* vol. 67, no. 11, pp. 9120–9132, Dec. 2020.

[19] G. Tan, Q. Deng, and Z. Liu, "An optimized SVPWM strategy for five-level active NPC (5L-ANPC) converter," *IEEE Trans. Power Electron.,* vol. 29, no. 1, pp. 386–395, Jan. 2014.

[20] Z. Liu, Y. Wang, G. Tan, H. Li, and Y. Zhang, "A novel SVPWM algorithm for five-level active neutral-point-clamped converter," *IEEE Trans. Power Electron.,* vol. 31, no. 5, pp. 3859–3866, May 2016.

[21] Q. A. Le and D.-C. Lee, "Reduction of common-mode voltages for five-level active NPC inverters by the space-vector modulation technique," *IEEE Trans. Ind. Appl.,* vol. 53, no. 2, pp. 1289–1299, Mar./Apr. 2017.
[22] Q. A. Le and D.-C. Lee, "Elimination of common-mode voltages based on modified SVPWM in five-level ANPC inverters," *IEEE Trans. Power Electron.,* vol. 34, no. 1, pp. 173–183, Jan. 2019.
[23] B. P. McGrath, D. G. Holmes, and T. Lipo, "Optimized space vector switching sequences for multilevel inverters," *IEEE Trans. Power Electron.,* vol. 18, no. 6, pp. 1293–1301, Nov. 2003.
[24] L. Lim, N. Ku, and D. Hyun, "A simplified space-vector PWM scheme for N-level NPC inverter based on two-level space-vector PWM," in *Proc. IEEE Veh. Power Propul. Conf.*, Oct. 2014, pp. 1–6.
[25] S. J. Hyeong, C. C. Ho, and H. D. Seok, "A new simplified space-vector PWM method for three-level inverters," *IEEE Trans. Power Electron.,* vol. 16, no. 4, pp. 545–550, Jul. 2001.
[26] L. Hang, B. Li, M. Zhang, Y. Wang, and L. M. Tolbert, "Equivalence of SVM and carrier-based PWM in three-phase/wire/level vienna rectifier and capability of unbalanced-load control," *IEEE Trans. Ind. Electron.,* vol. 61, no. 1, pp. 20–28, Jan. 2014.
[27] N. Oikonomou, C. Gutscher, P. Karamanakos, F. D. Kieferndorf, and T. Geyer, "Model predictive pulse pattern control for the five-level active neutral-point-clamped inverter," *IEEE Trans. Ind. Appl.,* vol. 49, no. 6, pp. 2583–2592, Nov./Dec. 2013.
[28] Y. Yang, J. Pan, H. Wen, Z. Zhang, Z. Ke, and L. Xu, "Double-vector model predictive control for single-phase five-level actively clamped converters," *IEEE Trans. Transport. Electrific.,* vol. 5, no. 4, pp. 1202–1213, Dec. 2019.
[29] D. Mukherjee and D. Kastha, "Carrier-based discontinuous PWM for a five-level unidirectional rectifier," *IEEE Trans. Power Electron.,* vol. 35, no. 6, pp. 5601–5614, Jun. 2020.
[30] S. R. Pulikanti and V. G. Agelidis, "Hybrid flying-capacitor-based active-neutral-point-clamped five-level converter operated with SHE-PWM," *IEEE Trans. Ind. Electron.,* vol. 58, no. 10, pp. 4643–4653, Oct. 2011.
[31] C. Li, S. Wang, Q. Guan, and D. Xu, "Hybrid modulation concept for five-level active-neutral-point-clamped converter," *IEEE Trans. Power Electron.,* vol. 32, no. 12, pp. 8958–8962, Dec. 2017.
[32] J. Pou, R. Pindado, D. Boroyevich, and P. Rodriguez, "Evaluation of the low-frequency neutral-point voltage oscillations in the three-level inverter," *IEEE Trans. Ind. Electron.,* vol. 52, no. 6, pp. 1582–1588, Dec. 2005.
[33] A. von Jouanne, S. Dai, and H. Zhang, "A multilevel inverter approach providing DC-link balancing, ride-through enhancement, and common-mode voltage elimination," *IEEE Trans. Ind. Electron.,* vol. 49, no. 4, pp. 739–745, Aug. 2002.
[34] X. Wu, G. Tan, Z. Ye, G. Yao, Z. Liu, and G. Liu, "Virtual-space-vector PWM for a three-level neutral-point-clamped inverter with unbalanced DC-links," *IEEE Trans. Power Electron.,* vol. 33, no. 3, pp. 2630–2642, Mar. 2018.
[35] S. Busquets-Monge, J. Bordonau, D. Boroyevich, and S. Somavilla, "The nearest three virtual space vector PWM-A modulation for the comprehensive neutral-point balancing in the three-level NPC inverter," *IEEE Power Electron. Lett.,* vol. 2, no. 1, pp. 11–15, Mar. 2004.
[36] J.-S. Lee and K.-B. Lee, "Time-offset injection method for neutral-point AC ripple voltage reduction in a three-level inverter," *IEEE Trans. Power Electron.,* vol. 31, no. 3, pp. 1931–1941, Mar. 2016.
[37] U.-M. Choi, F. Blaabjerg, and K.-B. Lee, "Method to minimize the low-frequency neutral-point voltage oscillations with time-offset injection for neutral-point-clamped inverters," *IEEE Trans. Ind. Appl.,* vol. 51, no. 2, pp. 1678–1691, Mar./Apr. 2015.
[38] A. K. Gupta and A. M. Khambadkone, "A simple space vector PWM scheme to operate a three-level NPC inverter at high modulation index including overmodulation region, with neutral point balancing," *IEEE Trans. Ind. Appl.,* vol. 43, no. 3, pp. 751–760, May/Jun. 2007.
[39] P. Liu, S. Duan, C. Yao, and C. Chen, "A double modulation wave CBPWM strategy providing neutral-point voltage oscillation elimination and CMV reduction for three-level NPC inverters," *IEEE Trans. Ind. Electron.,* vol. 65, no. 1, pp. 16–26, Jan. 2018.
[40] G. I. Orfanoudakis, M. A. Yuratich, and S. M. Sharkh, "Hybrid modulation strategies for eliminating low-frequency neutral-point voltage oscillations in the neutral-point-clamped converter," *IEEE Trans. Power Electron.,* vol. 28, no. 8, pp. 3653–3658, Aug. 2013.
[41] T. Wang, C. Chen, P. Liu, T. Liu, Z. Chao, and S. Duan, "A hybrid space-vector modulation method for harmonics and current ripple reduction of interleaved vienna rectifier," *IEEE Trans. Ind. Electron.,* vol. 67, no. 10, pp. 8088–8099, Oct. 2020.
[42] D. Mukherjee and D. Kastha, "Voltage sensorless control of VIENNA rectifier in the input current oriented reference frame," *IEEE Trans. Power Electron.,* vol. 34, no. 8, pp. 8079–8091, Aug. 2019.
[43] Y. Fu, N. Cui, J. Song, Z. Chen, C. Fu, and C. Zhang, "A hybrid control strategy based on lagging reactive power compensation for vienna-type rectifier," *IEEE Trans. Transport. Electrific.,* vol. 7, no. 2, pp. 825–837, Jun. 2021.

Peng Zhang received the B.S. degree in electrical engineering from the Anhui University of Technology, Anhui, China, in 2018. He is currently working toward the Ph.D. degree in electrical engineering with the School of Electrical Engineering, Beijing Jiaotong University, Beijing, China.

His current research interests include multilevel converters, dc-dc converters, and renewable power generation.

Xuezhi Wu (Member, IEEE) received the B.S. and M.S. degrees from Beijing Jiaotong University, Beijing, China, in 1996 and 1999, respectively, and the Ph.D. degree from Tsinghua University, Beijing, China, in 2003, all in electrical engineering.

He is currently an Associate Professor with the School of Electrical Engineering, Beijing Jiaotong University. His current research interests include micro grids, wind power generation systems, power converters for renewable generation systems, power quality, and motor control.

Wenzheng Xu received the B.Eng. degree in electrical engineering from Beijing Jiaotong University, Beijing, China, in 2012, the M.Sc. degree (with Distinction) in energy engineering from The University of Hong Kong, Hong Kong, in 2013, and the Ph.D. degree in electrical engineering from The Hong Kong Polytechnic University (PolyU), Hong Kong, in 2020.

From September 2013 to June 2015 and March to June 2020, he was a Research Assistant and a Postdoctoral Fellow, respectively, with the Department of Electrical Engineering, PolyU, working on high-power converters and fast-charging devices for electric vehicles. He is currently a Lecturer with the School of Electrical Engineering, Beijing Jiaotong University. His research interests include power electronics, wireless power transfer, transportation electrification, and energy interconnection.

Jingdou Liu received the B.S. and M.S. degrees in electrical engineering from Beijing Jiaotong University, in 1999 and 2006, respectively.

He is currently a Senior Engineer with the School of Electrical Engineering, Beijing Jiaotong University, Beijing, China. His current research interests include multilevel converters, power quality, and renewable power generation.

Jingjing Qi was born in Henan, China, in 1998. She received the B.S. degree in 2018 from Beijing Jiaotong University, Beijing, China, where she is currently working toward the Ph.D. degree in electrical engineering with the School of Electrical Engineering.

Her research interests include resonant converters and high-gain dc–dc converters.

Anna Yang received the B.S. degree in electrical engineering in 2019 from Beijing Jiaotong University, Beijing, China, where she is currently working toward the M.S. degree with the Department of Electrical Engineering.

Her current research interests include multilevel converters and high frequency inverters.